Influence of Material Surface Hardness and Particle Size on the Erosion of DC 11 Tool Steel
材料表面硬度及沖砂顆粒尺寸對 DC 11 工具鋼的沖蝕影響

Dong - Cherng Wen（溫東成）

Department of Mechanical Engineering, China Institute of Technology
中華技術學院機械工程系
NSC Project No. : NSC-92-2622-E-157-011-CC3

Abstract

The effect of surface hardness and particle size of erodent on the erosion behavior of DC 11 tool steel was examined by sand blasting. The hardness of the steel specimens was changed by case hardening of gas nitriding and vacuum heat treating. These samples were tested in an air jet impingement tester with a range of impact angles (15-90^o) and a particle velocity of 83.2m/s. Al_2O_3 sand particles having mean particle sizes of 115, 177 and 220μm. The results indicate that cutting is the dominated mode for material removal at oblique impact angle. At the higher impact angle, the mode is based on extrusion and cracking. At the medium impact angle, the wear is dominated by transition of mode mixed with cutting and extrusions. However, cracking is one of the major wear modes for all impact angles. The depth of cutting grooves or indentation craters of the treated samples is lower than that of normal samples. The maximum erosion rate in all cases shifts from oblique impact angle to medium impact angle with increasing hardness. They are at 15^o, 30^o and 45^o for normal, nitrided and vacuum heat treated samples, respectively. The erosion rates decrease with increasing hardness for all impact angles. The erosion rate for impinging with particle size of 177μm is larger than finer and coarser sized particles.

Keywords: erosion, surface hardness, particle size, tool steel

摘 要

本研究探討沖砂顆粒大小和材料表面硬度對 DC11 工具鋼沖蝕行爲的影響。試片施以氣體氮化和真空熱處理兩種硬化後，以未處理試片爲對照組作沖蝕試驗，Al_2O_3 砂粒沖蝕速度爲 83.2m/s，沖蝕角度爲 15-90^o，沖砂尺寸則爲 115, 177 和 220μm。結果顯示低角度沖蝕模式以斜向剪切爲主，高角度沖蝕模式爲擠壓與破裂，中等角度沖蝕則混合有斜向剪切與擠壓兩種模式。硬化處理後試片的剪切或擠壓深度都較未處理試片淺。而隨硬度增加，最大沖蝕速率由低角度件增至中等角度，又各沖蝕角度的沖蝕速率也會隨硬度增加而減少，三種沖砂尺寸則以中等顆粒 (177μm)的沖蝕速率較大。

關鍵詞：沖蝕，表面硬度，沖砂尺寸，工具鋼。

1. Introduction

DC 11 tool steel is a general-purpose cold work die and mold steel whose strength and toughness approach those of high-speed steels. It is extensively used for mold in the metal forming or plastic injection industries. Moreover, this steel is generally heat treated to provide moderate wear resistance and a good combination of mechanical properties. This treatment often involves a harden treating. After tempering at certain temperature, both strength and toughness are higher than that of SKD 11 steel. Solid particle erosion rates of metals have been reported to be relatively insensitive to prior hardening effect[(1)]. Improving the erosion wear of materials requires an understanding of the mechanism by which the material is removed.

Two models have been employed to describe the erosion behavior for ductile materials and brittle materials respectively. Ductile materials during erosion are considered to lose material via a cutting mechanism at a low impact angle in the erosion rate as a function of the impact angle[(2)].On the other hand, the erosion damage of brittle materials is based on cracking and occurs at impact angle closed to norma[(3)]. The resolved shear stress of particle impact provides the force for cutting, boundary cracking of materials, and eroding away of pieces[(4-6)]. The resolved normal stress provides the force for lipping, ridging, cratering, surface and sub-surface cracking. However, the cutting mechanism is only valid at oblique impact angle.

Erosion wear usually occurs if the particle hardness is greater than the material hardness[7]. The improvement in the hardness with ductility of the material results in increased resistance to erosion[8]. The effects of harden effect on erosion rate have been discussed in detail. Naim and Bahadur[9] reported that a higher erosion rate was observed for both the oblique and the normal impact conditions due to an increase in cold working. Bregliozzi [10] investigated the cavitation wear of austenitic stainless steels with different grain size. He concluded that the resistance to cavitation erosion increases with decreasing grain size. Korshunov[11] reported an increase of 2-5 times in abrasive sliding wear resistance of quenched and tempered steel when the grain size of steel was reduced from 100 to 10μm. Molian et al[12] compared the erosion rate of untreated sample with laser heat treated sample. They revealed that the erosion rates of laser heat treated sample was substantially lower than that of untreated sample and they also found that the material removal is through micro machining and ploughing in untreated condition and through intergranular cracking in laser heat treated condition. However, there is little work reported in the literature on the influence of nitriding and vacuum heat treating on the particle erosion of tool steels like DC 11. Thus, this study was undertaken to examine the potential of surface harden effect on the erosion behavior of DC 11 tool steel. Also investigated is the correlation between erosion rate and a wide range of operating parameters such as impact angle and mean particle size.

2. Experimental Procedures

2.1.Material preparation and heat treatment

The target material for this study is DC 11 tool steel. The chemical composition of the experimental material is listed in Table 1. The steels were cut into 50mm×35mm×6mm shapes for erosion tests and dimension 20mm×20mm×6mm for metallographic examination and hardness tests. These specimens are annealed in as received. The fresh untreated specimen is referred to as "normal sample" in this work. Hardness of the specimens was increased to two levels by vacuum heat treating and case hardening by gas nitriding. The vacuum heat treating is processed with austenitizing at 1030℃ for 1hr and than tempering at 520℃ for another 1 hr.

Table 1 Chemical composition of experimental material. (wt%)

C	Cr	Si	Mn	Mo	V	Ni	Fe
0.91	121.05	0.26	0.34	0.89	0.23	0.54	Bal.

2.2. Erosion tests

After the above heat treatments, the normal sample and treated samples were subjected to erosion wear test. The erosion tests were conducted in a typical sand-blast type of test rig with a ϕ5mm size nozzle. The Al_2O_3 sand with mean particles sizes of 115, 177 and 220μm and irregular in shape were used as the erodent. Erodent particles were fed to the test rig at a constant rate of 600g/min by using a pressurized carrier gas. The erosion velocity at a distance from the nozzle tip of 30mm was 83.2 m/s estimated by a single-shot high-speed photography. The erosion stream being directed to impinge in the sample surface at different angles of 15^o, 30^o, 45^o, 60^o, and 90^o; while the amount of erosion particles was 6000g for each experience run. For every new experiment, a fresh batch of sand was used. Each erosion datum was the average of at least three test results. The samples were ultrasonically cleaned in acetone before weighting.

2.3. Metallography and Hardness Test

After polishing and etching with Nital reagent, the metallography specimens were used to examine the microstructure by utilizing scanning electron microscopy (SEM) and optical microscopy. SEM was also applied to observe the surface and subsurface of the eroded specimens for the evaluation of the fracturing mode. Hardness testing of the substructure and surface of the experimental material were performed using standard Vickers (100g) and Rockwell hardness testers, respectively. Before testing, the specimens were polished and etched in the same way as for the metallographic examination. All the Rockwell hardness readings were converted to Vickers hardness numbers. At least five hardness readings were taken, and then averaged.

3. Results and Discussion

3.1. Microstructures and Hardness

Figure 1 shows the microstructure of the normal and treated samples. It consists of martensite and carbide. The size of carbide in the normal sample (Fig. 1(a)) is small than that in the treated samples. After gas nitriding, larger amount of extremely small uniformly carbides were precipitated resulting in increasing the surface hardness (Fig. 1(b)). During vacuum heat treating, the high temperature of austenitizing leads the solid solution of alloy and carbide. This caused the matrix become martensite. After tempering, the precipitation of larger size of carbides contributes a secondary hardening effect (Fig. 1(c)).The hardness of the normal and treated samples are listed in Table 2.

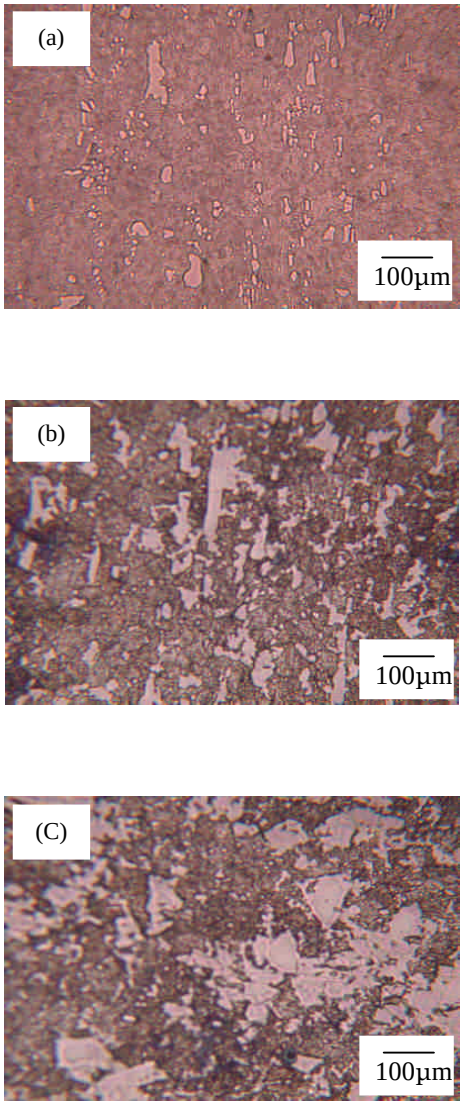

Fig. 1.The microstructure of the normal and treated samples. (a) normal, (b) nitriding, and (c) vacuum heat treating.

Table 2 The hardness of the normal and treated samples. (HRc)

Sample	Substructure	Surface
Normal	23.5	23.5
Nitriding	55.7	67.3
Vacuum. heat treating	72.7	72.7

3.2. Examination of eroded samples

The worn surfaces of any given impact angles for all samples impinging at three different particle size have a similar characteristic, only the samples impinged with particle size of 177µm were discussed here. The worn surfaces of the normal samples are shown in Fig. 2. The surface of low impact angle (15^o) sample shows long and narrow groove, in which cutting chips and some surface cracks can be found (Fig. 2(a)). The surface of the sample at the impact angle of 45^o shows a mixture of cutting groove and extrusion crater (Fig. 2(b)). Erosion tests at 60^o and 90^o reveal extrusion of lips and cracks, where the deformation zone goes along with the side of lips also presented but cutting mode is absent (Fig. 2(c)). It is therefore reasonable to summarize that cutting is the dominated mode for material removal at oblique impact angle. In this case, the morphology of the surface damage is long and shallow cutting grooves. At the higher impact angle, the mode is based on extrusion and cracking. However, at the medium impact angle, the wear is dominated by transition of mode mixed with cutting and extrusions. Both features of grooves and indentation craters are observed. However, cracking is one of the major wear modes for all impact angles.

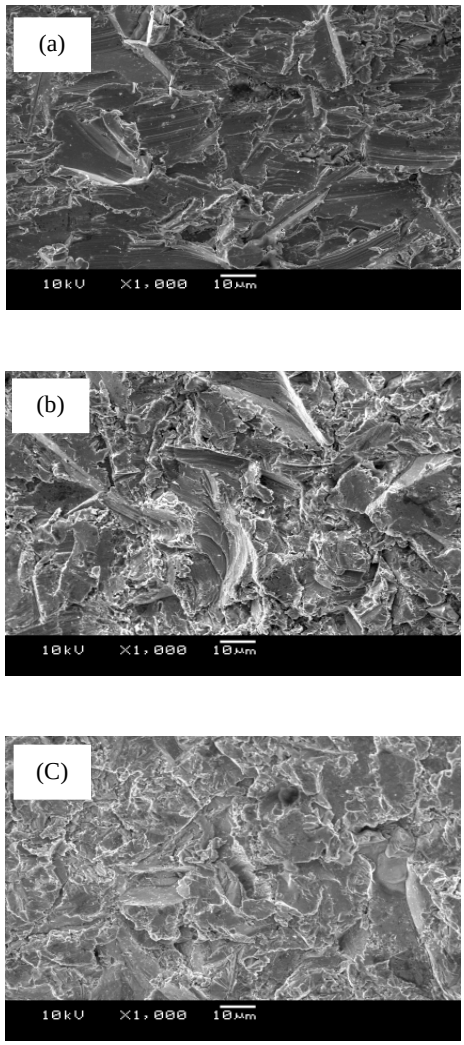

Fig.2. SEM micrographs showing the worn surfaces of the normal samples after impinging with particle size of 115m and variant impact angle (a) 15^o, (b) 45^o, and (c) 90^o.

The worn surfaces of the nitriding (Fig. 3) and vacuum heat treating samples (Fig. 4) are similar to the worn surfaces of the normal samples. However, the depth of cutting grooves or indentation craters of the treated samples is lower than that of normal samples because the hardness is increased after treating. The effects of wear mode, particle size and hardness on erosion rate were further discussed in the following section.

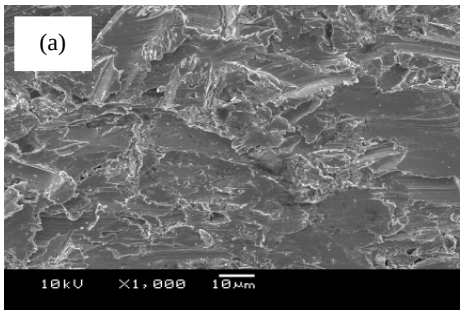

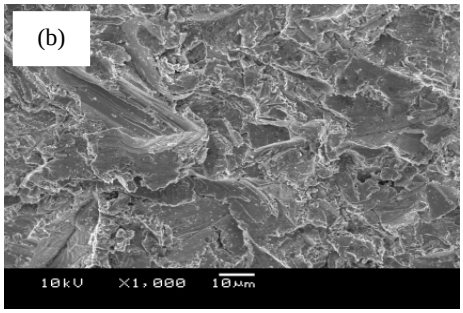

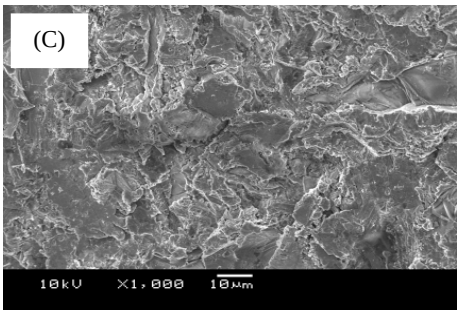

Fig.3. SEM micrographs showing the worn surfaces of the nitrided samples after impinging with particle size of 177µm and variant impact angle (a) 15^o, (b) 45^o, and (c) 90^o.

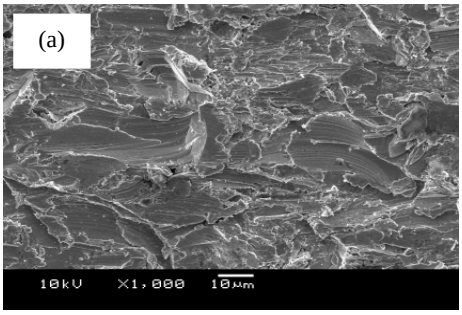

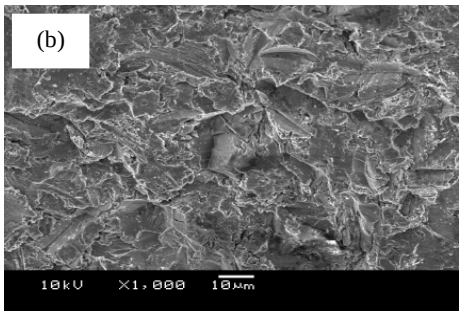

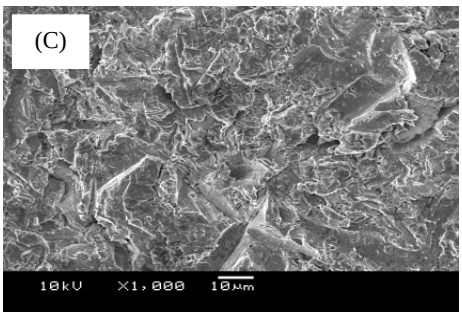

Fig.4 SEM micrographs showing the worn surfaces of the vacuum heat treated impinging with particle size of 220µm and variant impact angle (a) 15^o, (b) 45^o, and (c) 90^o.

3.3. Erosion data

The results of erosion test impinging with particle size of 115µm versus the impact angle for samples of varying hardness are shown in Fig. 5. Figs. 6 and 7 show similar results for a particle size of 177 and 220 µm.

It is clear from the results that the increased hardness has resulted in lower erosion rates. Because increasing in hardness provides resistance to penetration and, result in lower erosion rate. The maximum erosion rate in all cases shifts from oblique impact angle to medium impact angle with increasing hardness. They are at 15^o, 30^o and 45^o for normal, nitrided and vacuum heat treated samples, respectively.

The maximum erosion rate of normal sample at lower impact angle is typical ductile material erosion model. After heat treating, increasing in hardness causes the erosion mixture with ductile and brittle models. As a consequence, the angle of maximum erosion rate increases to 30^{o}-45^{o}. When the effect of particle size is considered, the erosion rates decrease with increasing particle size for all impact angles.

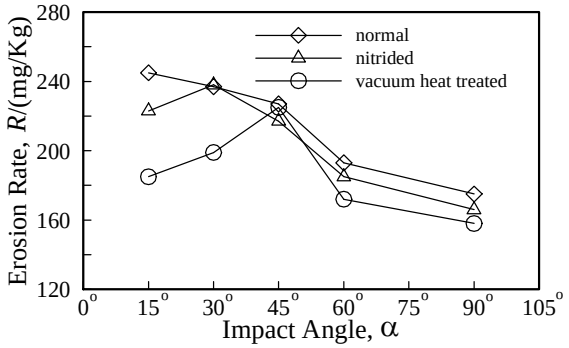

Fig. 5. Erosion rate with respect to impact angle for normal and treated samples (particle size : 115 μm).

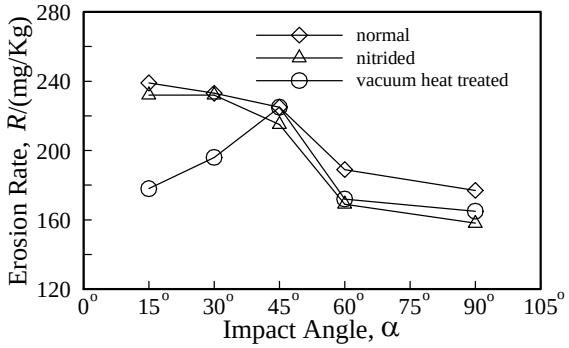

Fig. 6. Erosion rate with respect to impact angle for normal and treated samples (particle size : 177 μm).

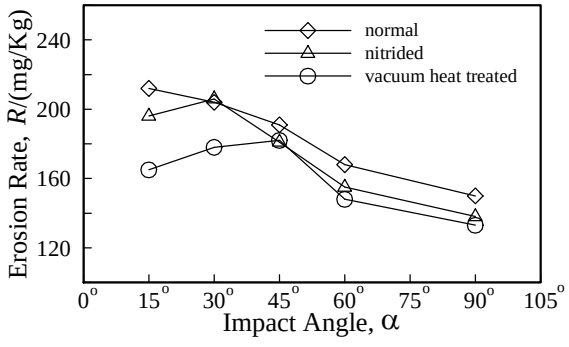

Fig. 7. Erosion rate with respect to impact angle for normal and treated samples (particle size : 220 μm).

The relationship between the maximum erosion rate of the experimental materials and their surface hardness is shown in Fig.8. The ability of resistance to penetration for normal sample is lower due to its lower hardness, therefore, having the highest erosion rate. For nitriding sample, the hardness of substructure is lower than that of vacuum heat treating sample even the surface hardness is close to that of vacuum heat treating samples. Hence, the maximum erosion rate of nitriding sample is larger than that of vacuum heat treating sample.

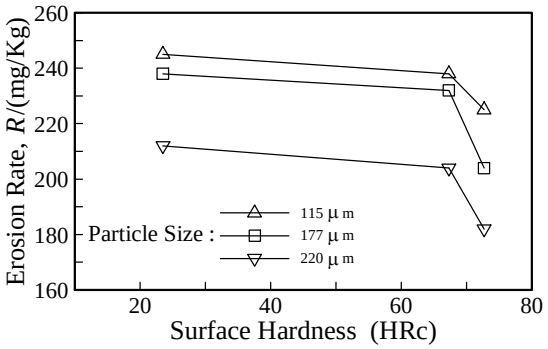

Fig. 8. Maximum erosion rate as a function of hardness.

The maximum erosion rate as a function of particle size is shown in Fig. 9. For all samples, the maximum erosion rate decrease with increasing particle size of erodent. For a given mass of particles the number of particles will reduce as the particle size increases. Thin means that the in case of larger size particles, for a given mass, the number of particles impinging on the target would be less than the fine sized particles. On the other hand, the particle velocity for coarser particles would be lower than those of finer sized particles. The combined effect of the number of particles and the kinetic energy may result in lower erosion rate for the coarser particles.

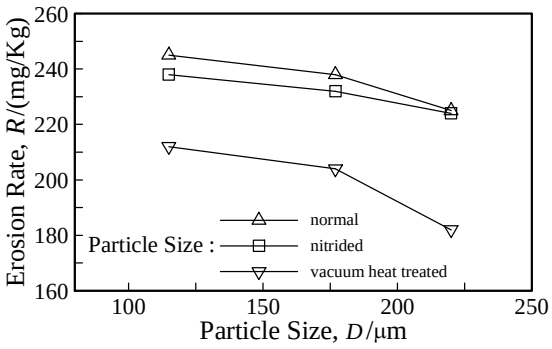

Fig. 9. Maximum erosion rate as a function of particle size.

4. Conclusions

The effect of surface hardness and particle size of erodent on the erosion behavior of DC 11 tool steel was studied. The following conclusions are drawn.

(1) For all cases, cutting is the dominated mode for material removal at oblique impact angle. At the higher impact angle, the mode is based on extrusion and cracking. At the medium impact angle, the wear is dominated by transition of mode mixed with cutting and extrusions. Both features of grooves and indentation craters are observed. However, cracking is one of the major wear modes for all impact angles. The depth of cutting grooves or indentation craters of the treated samples is lower than that of normal samples.

(2) The maximum erosion rate in all cases shifts from oblique impact angle to medium impact angle with increasing hardness. They are at 15^{o}, 30^{o} and 45^{o} for normal, nitrided and vacuum heat treated samples, respectively.

(3) The nitriding and vacuum heat treating improved the erosion resistance of DC 11 tool steel by increasing its hardness. Because increasing in hardness provides resistance to penetration and, result in lower erosion rate.

(4) The maximum erosion rate decrease with increasing particle size of erodent. In case of large size particle, for a given mass, the number of particles impacting on the surface would be less than the fine sized particles. The particle velocity for coarser particles also would be lower than those of finer sized particles. The combined effect of the number of particles and the kinetic energy may result in lower erosion rate for the coarser particles.

REFERENCES

(1) G. Sundararajan and P. G. Shewmon: A New Model for the Erosion of Metals at Normal Incidence, Wear, 84, 1983, pp.237-258.

(2) G. L. Sheldon, K. Kanhere: An Investigation of Impingement Erosion using Single Particles, Wear, 21, 1972, pp.195-209.

(3) I. Finnie: Erosion of Surfaces by Solid Particles, Wear, 3, 1960, pp.87-103.

(4) Y. I. Oka, H. Ohnogi, T. Hosokawa and M. Matsumura: The Impact Angle Dependence of Erosion Damage Caused by Solid Particle Impact, Wear, 203-204, 1977, pp.573-579.

(5) I. Finnie and D. H. McFadden: On the Velocity Dependence of the Erosion of Ductile Metals by Solid Particles at Low Angles of Incidence, Wear, 48, 1978, pp.181-190.

(6) J. G. A. Bitter: A Study of Erosion Phenomena: Part II, Wear, 6, 1963, pp. 169-190.

(7) A. A. Torrance: An Explanation of the Hardness Differential Needed for Abrasion, Wear, 68, 1981 pp.263-266.

(8) K. C. Goretta, R. C. Arroyo, C. T. Wu and J. L. Routbort: Erosion of Work-Hardened Copper, Nickel, and 304 Stainless Ssteel, Wear, 147, 1991, pp.145-154.

(9) M. Naim and S. Bahadur: The Significance of the Erosion Parameter and the Mechanisms of Erosion in Single-Particle Impacts, Wear, 94, 1984, pp.219-232.

(10) G. Bregliozzi, A. Di Schino, S. I. U. Ahmed, J. M. Kenny and H. Haefke: Cavitation Wear Behaviour of Austenitic Stainless Steels with Different Grain Sizes, Wear, 258, 2005 pp.503-510.

(11) L. G. Korshunov, A. M. Polyakova and N. L. Chrnenko: Umova Vm. Phys. Met. Metallogr. 61 (1986) 160-67.

(12) P. A. Molian and Mark Baldwin: Effects of Single-Pass Laser Heat Treatment on Erosion Behavior of Cast Irons, Wear, 118, 1987, pp.319-327.